Goldstone-like States in a Layered Perovskite with Frustrated Polarization: A First-Principles Investigation of $PbSr_2Ti_2O_7$

S. M. Nakhmanson
Materials Science Division, Argonne National Laboratory, Argonne, Illinois 60439, USA

Ivan Naumov
Hewlett-Packard Information and Quantum Systems Laboratory, 1501 Page Mill Road, Palo Alto, California 94304, USA
(Received 23 October 2009; published 4 March 2010)

With the help of first-principles-based computational techniques, we demonstrate that Goldstone-like states can be artificially induced in a layered-perovskite ferroelectric compound with frustrated polarization, resulting in the emergence of a variety of interesting physical properties that include large, tunable dielectric constants and an ability to easily form vortex polar states in a nanodot geometry. In a similar fashion to the well-known perovskite materials with morphotropic phase boundaries (MPBs), these states manifest themselves as polarization rotations with almost no energy penalty, suggesting that the existence of an MPB is actually yet another manifestation of the Goldstone theorem in solids.

DOI: 10.1103/PhysRevLett.104.097601 PACS numbers: 77.84.−s, 63.20.dk, 63.22.Np, 81.05.Zx

Identifying and manufacturing compounds with morphotropic phase boundaries (MPBs) is one of the most important problems related to the physics and applications of electroactive materials. Such compounds must be tuned into a specific area within their phase space where a small external influence (e.g., elastic or electric field) triggers a phase transition accompanied by a large change of the system's polarization. This usually happens via the rotation of the polarization vector $\mathbf{P}$ between the two crystallographic directions and is essential for attaining colossal electroactive properties that are critically important for modern state-of-the-art technological applications [1–5]. Currently, MPB engineering is achieved by precisely controlling the composition of solid-solution or relaxor ferroelectrics [2,6]. However, in the words of Ref. [5], this results in materials that are ''usually complex, engineered, solid solutions, which complicates their manufacture as well as introducing complexity in the study of the microscopic origins of their properties.'' Furthermore, this statement perfectly summarizes the problems that arise in predictive computational studies of such structures utilizing, e.g., density-functional theory (DFT) methods, which are currently a tool of choice for the design of better, more efficient materials and nanostructures.

In this Letter, we outline an original approach for creating conceptually and structurally simple electroactive materials with an MPB (or a functional equivalent) built in by construction, with no need for alloying or application of negative pressure [5]. This approach exploits the celebrated Goldstone theorem [7], which in its nonrelativistic form states that breaking of a continuous-symmetry element in a system gives rise to a massless excitation with frequency $\omega \rightarrow 0$ for a wave vector $\mathbf{k} \rightarrow \mathbf{0}$ that ''on average'' restores the lost continuous symmetry. Although a few examples of such Goldstone modes are known in isotropic solids, including Heisenberg ferromagnets [8], liquid crystals [9], and incommensurate structures [10], in regular crystals, which are usually highly anisotropic, such modes are extremely rare. Superconducting $Cd_2Re_2O_7$ [11] is the only well-documented example, where the effective Hamiltonian of the soft-phonon mode is nearly isotropic due to the material's peculiar symmetry [12], with the first nonzero anisotropic term appearing only as a *sixth-order* invariant composed of the components of the (doubly degenerate) mode's order parameters.

In what follows, we show that light [$\omega(\mathbf{k} = \mathbf{0}) \sim 0$], Goldstone-like excitations can be induced even in systems with ''less forgiving'' symmetry, where lower-order anisotropic invariants in the soft-mode's effective-Hamiltonian expansion do not cancel out exactly [13]. We prove that such low-order energy anisotropies can, nevertheless, be tuned out if they are strongly coupled with certain external thermodynamic parameters that we can conveniently manipulate. Specifically, we utilize DFT methods to predict that Goldstone-like states exist in an artificial Ruddlesden-Popper (RP [14])-type superlattice $PbSr_2Ti_2O_7$, where two-dimensional fragments of an *A*-site driven [15] perovskite ferroelectric $PbTiO_3$ are alternated with nonferroelectric SrO layers (Fig. 1). We demonstrate that, in spite of their reduced dimensionality, these fragments still undergo polar distortions driven by the hybridization between the lead 6*s* and oxygen 2*p* states, and that the resulting energy landscapes can be made highly isotropic by applying epitaxial strain. This, in turn, gives rise to easy (i.e., incurring almost no energy costs), Goldstone-like in-plane rotations of polarization [1] in the system's state with broken symmetry, making it behave in the same fashion as a material with a built-in MPB.

We begin the discussion by describing the structure of $PbSr_2Ti_2O_7$ (PSTO in what follows) and commenting on the technical details of the calculations. A tetragonal unit cell containing two structural $PbSr_2Ti_2O_7$ units (s.u.) and

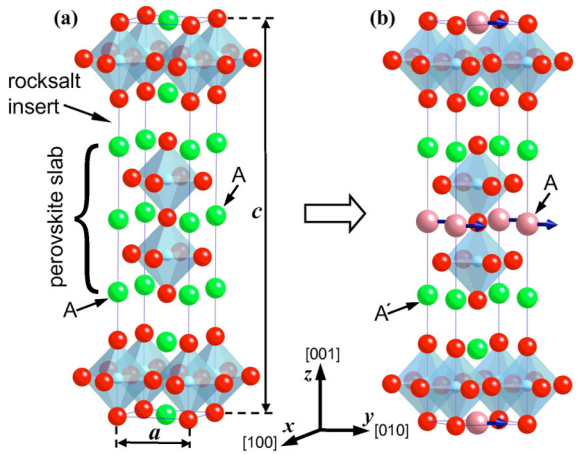

FIG. 1 (color online). Crystal structure of $n = 2$ RP compounds: (a) $Sr_3Ti_2O_7$; the lattice constants for the tetragonal cell are also shown. (b) $PbSr_2Ti_2O_7$ RP superlattice obtained from the structure (a) by assigning different A-site ions to the perovskite and rocksalt units. An in-plane ferroelectric distortion of the superlattice, consisting mostly of displacements of the lead atoms, is outlined by bold arrows. TiO_6 cages are represented by translucent octahedra, Sr atoms are shown in green (dark gray) and Pb atoms in pink (light gray).

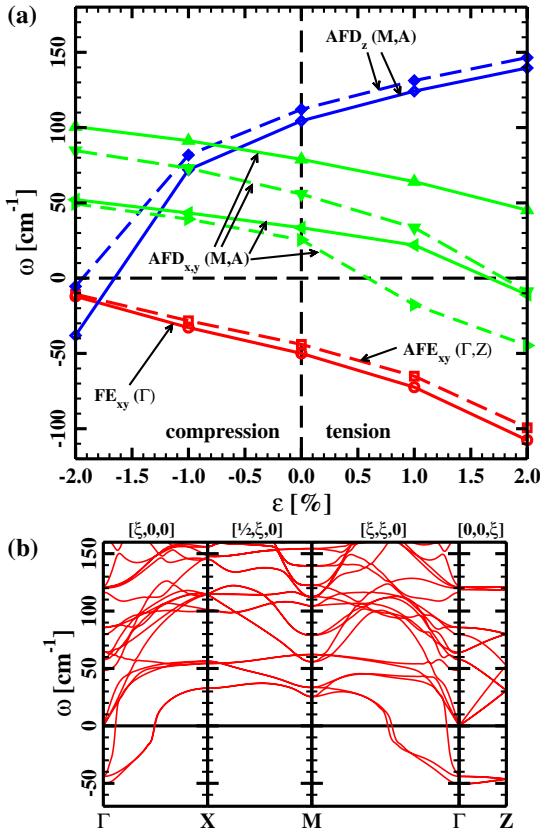

FIG. 2 (color online). (a) Soft-mode frequencies ω at Γ and various BZ-boundary $\mathbf{k}$ points (marked in brackets) versus epitaxial strain $\varepsilon = a/a(\varepsilon = 0) - 1$ for PSTO. Instability label subscripts indicate the sense of direction: axial (α) or planar ($\alpha\beta$) ionic motion for the FE and AFE ones, single (α) or an equivalent set (α, β) of rotational axes for the AFD ones; here, $\alpha, \beta = x, y, z$. $\omega(\varepsilon)$ dependencies at different $\mathbf{k}$ points that have degenerate or nearly degenerate frequencies are shown by the same curves. (b) Phonon-band dispersions along certain high-symmetry BZ directions in the unstrained PSTO.

characterized by the in-plane lattice constant a, and out-of-plane lattice constant c is shown in Fig. 1, and was used in all the calculations presented below. A plane-wave DFT-based method [16] with ultrasoft pseudopotentials [17] was employed for the relaxation of ionic positions in the cell (with $4/mmm$ symmetry enforced), after which the phonon frequencies were computed across the tetragonal Brillouin-zone (BZ) with the help of a density-functional perturbation theory approach [18].

We have recently identified PSTO as a structure exhibiting only ferroelectric (FE) and antiferroelectric (AFE) instabilities while being free of any antiferrodistortive (AFD) ones, which involve tilting of octahedral oxygen cages and could potentially diminish or even destroy polarization [19]. This picture is unchanged by an epitaxial matching of PSTO to cubic (c-) $SrTiO_3$, since that generates only a 0.1% compressive strain [19]. The results of the structural-instability analysis of the $I4/mmm$ PSTO for a wider range of epitaxial strains—from 2% tension to 2% compression, which are routinely achieved during growth of high-quality perovskite-FE thin films—are presented in Fig. 2. As shown in panel (a), the presence of the rocksalt-type inserts in PSTO destroys any polar instabilities oriented along z. This effectively turns the system into a stack of polarized PbO planes [see Fig. 1(b) for a sketch of the $FE_{xy}(\Gamma)$ distortion], since for all the strains except for compressions of $\sim$2%, the AFD modes are pushed out to higher frequencies, and the ground state is set by freezing in of the soft in-plane FE and AFE modes. The polarized planes interact with each other quite weakly because of the near degeneracy of the $FE_{xy}(\Gamma)$, $AFE_{xy}(\Gamma)$, and $AFE_{xy}(Z)$ instabilities. This tendency is confirmed by tracking the dispersion of these modes along the Γ–Z line in the BZ—as shown in Fig. 2(b) for the unstrained system—which remains very flat for all the considered strains.

Since both the $FE_{xy}(\Gamma)$ and $AFE_{xy}(\Gamma)$ distortions are doubly degenerate (both transform according to the E_u irrep), potentially any linear combination of these instabilities could freeze in in the transition from the high-temperature paraelectric $I4/mmm$ phase to a low-temperature polar phase with reduced symmetry. To determine the polarization direction of the latter, we have sampled the energy landscapes of the system with respect to these distortions. Combinations of the modes' eigenvectors polarized along the x and y axes were frozen in with varying amplitudes Q_x and Q_y, and the energies of the resulting structures were computed on a 15×15 square amplitude grid. The energy surfaces for the unstrained (or, equivalently, strained on c-$SrTiO_3$) system are shown in

Fig. 3. Surprisingly, for both the FE [panel (a)] and AFE [panel (b)] distortions, they look very isotropic, lacking well-defined minima for any particular polarization directions. Instead, continuous, circularly shaped minimum-energy paths are present at $|\mathbf{Q}| = \sqrt{Q_x^2 + Q_y^2} \cong 9.5\%a$ for the FE and $7.0\%a$ for the AFE distortions. Energy corrugations sampled on a dense grid of points along these paths are smaller than 1 meV/s.u. for the "frozen" and 2 meV/s.u. for relaxed polar configurations [20]. In the polarized systems, $|\mathbf{P}| = 0.22$ C/m^2 for the one with $\mathbf{P} \parallel [100]$ and 0.21 C/m^2 for the one with $\mathbf{P} \parallel [110]$. Phonon-band calculations repeated for both systems demonstrate that the former one is stable, with no soft modes present anywhere in the BZ, and the latter has two soft modes at Γ-point (with the frequencies of $28i$ and $23i$ cm^{-1}) corresponding, respectively, to the in-phase and out-of-phase rotations of $\mathbf{P}$ away from the [110] direction in the two PbO planes in the simulation cell.

We have also computed the energy surfaces for frozen in $FE_{xy}(\Gamma)$ and $AFE_{xy}(\Gamma)$ distortions in the epitaxially strained versions of PSTO (not shown), whose shapes and energy-minima locations exhibit strong dependence on the applied strain. For $0 \geq \varepsilon \geq -1\%$, similarly to the situation visualized in Fig. 3, the surfaces remain mostly isotropic, and continuous minimum-energy paths persist. For stronger compressive strains, these paths become very shallow and collapse into the point of origin, indicating that the $I4/mmm$ phase is no longer unstable against polar distortions—but not against the AFD ones that soften up dramatically at such compressions, as shown in Fig. 2(a). On the other hand, when tensile strains are applied, continuous paths disappear in favor of discrete energy minima localized along the [110] direction. The latter is a much more conventional scenario, common for most epitaxially stretched FE perovskites.

To understand why there is no well-defined angular preference for developing in-plane polarization in the $I4/mmm$ PSTO at particular epitaxial strains, we have examined the individual components of the vibrational eigenvectors associated with the $FE_{xy}(\Gamma)$ and $AFE_{xy}(\Gamma)$ modes and evaluated the system's stability with respect to in-plane polar distortions localized only in PbO or TiO_2 layers. This analysis shows that in FE-distorted PSTO, the rocksalt SrO inserts act as braces on Ti ions in the neighboring layers, completely preventing them from moving away from the centrosymmetric positions in their octahedral cages. Thus, the system's polarization emerges *exclusively* due to large off centering of lead ions in their 12-fold cuboctahedral cages. I.e., PSTO can be considered as an *A*-site driven ferroelectric "distilled" into its purest form [15]. The frustration of the system's polarization, namely, its inability to have a component along [001], enforces a competition between the [100]; and [110] directions for the developing FE distortions, which could be conceptually regarded as the tetragonal and rhombohedral phase analogs in a material with an MPB. At high tensions, the [110] energy minimum becomes deeper with the polarization locking itself in along this direction, while at high compressions, there is a slight preference for the [100] direction, before the system becomes paraelectric. However, there is a favorable strain interval in between these states when the cuboctahedral lead-ion cage becomes highly isotropic, with the energy minima for FE distortions along [100] and [110] having approximately the same depth, and their basins of attraction coalescing, thus forming a circularly shaped minimum-energy trench [21].

The Goldstone-like (optical) excitations that manifest themselves in the low-symmetry FE-distorted phases as easy polarization rotations inside this trench provide the largest contributions to the diagonal components of the system's in-plane static dielectric susceptibility tensor. In the [100] and [110] FE-distorted variants studied, these are found to be as large as 430 and could potentially be attuned to even higher values by adjusting the epitaxial strain and making the system's energy landscape as isotropic as possible. Additionally, the absence of the preferable direction for polarization indicates that PSTO will easily adopt a *vortex* (or toroidal) dipole ordering [22] when shaped into a

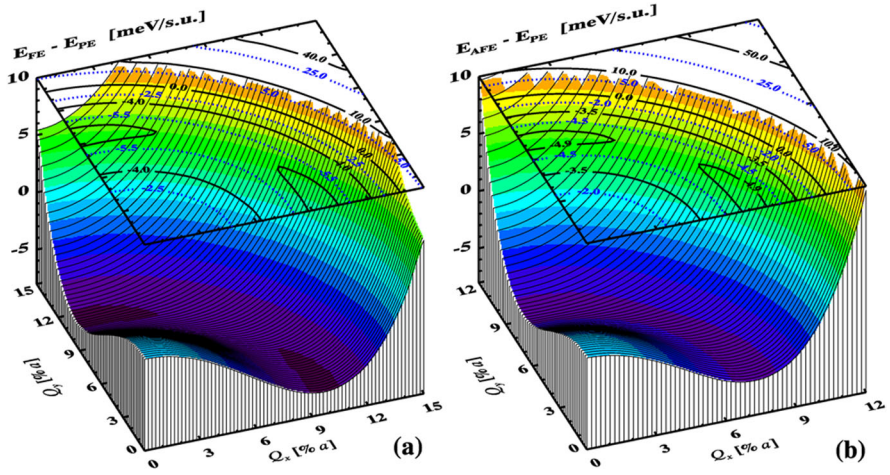

FIG. 3 (color online). Energy landscapes for the unstrained $I4/mmm$ PSTO system with frozen-in doubly degenerate (a) FE_{xy} and (b) AFE_{xy} distortions. Q_x and Q_y are the amplitudes of the modes' eigenvectors polarized along the x and y axes, respectively. The energy of the paraelectric $I4/mmm$ phase is taken as zero and a is the value of the in-plane lattice constant.

nanodisk or other flat nanoparticle. Such vortex states are very promising for memory applications due to a projected several orders of magnitude increase in storage density [22].

On the electronic level, the driving force for the $FE_{xy}(\Gamma)$ and $AFE_{xy}(\Gamma)$ distortions is the rehybridization of the lead $6s$ band with the oxygen $2p_x$ and $2p_y$ bands in the PbO planes, which leads to the widening of the optical gap and lowering of the total energy. In the $I4/mmm$ phase, Pb and O atoms form a highly symmetrical square CsCl-type lattice, with the energy gain due to the polar distortion being almost independent of its direction. Likewise, in pure lead oxide, the same chemical interactions produce a variety of distorted polymorphic structures [23], including some incommensurate ones [24]. Work to understand the exact underpinnings of such directional degeneracy of orbital interactions is currently underway. We should also point out that for the lead-based RP superlattices, the appearance of Goldstone-like polarization rotations is possible only in $PbSr_2Ti_2O_7$, i.e., a structure with just one PbO layer per perovskite slab. As shown in Fig. 2(c) of Ref. [19], the following members of the series are highly prone to AFD_z instabilities that disrupt the in-plane polar order.

We believe that PSTO would lend itself well to molecular-beam epitaxy (MBE) growth, since a number of RP materials with varying n [25], including a superlattice [26], as well as other related structures [27] had been manufactured by this technique. We, nevertheless, realize the complications involved in conducting MBE with lead and are currently on a lookout for a lead-free material that would exhibit similar behavior. This will also allow us to estimate how forgiving our recipe for creating materials with Goldstone-like excitations is to varying identities of atomic species and whether the emergent interesting properties are indigenous to lead's chemistry and/or A-site ferroelectricity, or if they can be reproduced in other structures with frustrated polarization.

This project was supported by the U.S. Department of Energy, Office of Science, Office of Basic Energy Sciences under Contract No. DE-AC02-06CH11357. S. M. N. is grateful to Brian Stephenson and Ram Seshadri for fruitful discussions.

[1] H. Fu and R. E. Cohen, Nature (London) **403**, 281 (2000).
[2] R. Guo *et al.*, Phys. Rev. Lett. **84**, 5423 (2000).
[3] B. Noheda, Curr. Opin. Solid State Mater. Sci. **6**, 27 (2002).
[4] Z. Wu and R. E. Cohen, Phys. Rev. Lett. **95**, 037601 (2005).
[5] M. Ahart *et al.*, Nature (London) **451**, 545 (2008).
[6] S.-E. Park and T. R. Shrout, J. Appl. Phys. **82**, 1804 (1997).
[7] J. Goldstone, A. Salam, and S. Weinberg, Phys. Rev. **127**, 965 (1962).T. Schneider and P. F. Meier, Physica **67**, 521 (1973).
[8] P. M. Chaikin and T. C. Lubensky, *Principles of Condensed Matter Physics* (Cambridge University Press, Cambridge, 1995).
[9] I. Muševič, R. Blinc, and B. Žekš, *The Physics of Ferroelectric and Antiferroelectric Liquid Crystals* (World Scientific, Singapore, 2000).
[10] A. D. Bruce and R. A. Cowley, *Structural Phase Transitions* (Taylor and Francis Ltd., London, 1981).
[11] C. A. Kendziora *et al.*, Phys. Rev. Lett. **95**, 125503 (2005); J. C. Petersen *et al.*, Nature Phys. **2**, 605 (2006).
[12] I. A. Sergienko and S. H. Curnoe, J. Phys. Soc. Jpn. **72**, 1607 (2003).
[13] Like for most perovskites, for the material considered here, the first nonzero anisotropic invariant is of fourth order.
[14] S. N. Ruddlesden and P. Popper, Acta Crystallogr. **10**, 538 (1957); **11**, 54 (1958).
[15] M. Ghita *et al.*, Phys. Rev. B **72**, 054114 (2005); D. J. Singh *et al.*, Ferroelectrics **338**, 73 (2006).
[16] Quantum Espresso, http://www.quantum-espresso.org/. Local-density approximation was used to account for exchange and correlations. A $6 \times 6 \times 2$ mesh [H. J. Monkhorst and J. D. Pack, Phys. Rev. B **13**, 5188 (1976)] was employed for the BZ integrations and for phonon-band calculations. To simulate the influence of epitaxial strain, a was constrained to a number of different values while c was allowed to vary. The system was considered to be at equilibrium when ionic forces were less than 0.01 eV/Å and the σ_{zz} component of the stress tensor was smaller than 0.2 KBar.
[17] D. Vanderbilt, Phys. Rev. B **41**, 7892 (1990).
[18] S. Baroni *et al.*, Rev. Mod. Phys. **73**, 515 (2001).
[19] S. M. Nakhmanson, Phys. Rev. B **78**, 064107 (2008).
[20] Both the ionic forces and the σ_{zz} were relaxed again to the tolerances described above [16] in the structures with FE distortions induced along [100] ($Imm2$) and [110] ($Fmm2$). For all other directions, the symmetry is too low to restrict the polarization to the chosen direction during the relaxation.
[21] The interval of simulated strains is wide enough to ensure that any small errors in the determination of lattice parameters (e.g., due to the limitations of the accuracy of the DFT techniques) will not result in a complete disappearance of the Goldstone-like polarization rotations in PSTO.
[22] I. I. Naumov, L. Bellaiche, and H. Fu, Nature (London) **432**, 737 (2004); I. Naumov and A. M. Bratkovsky, Phys. Rev. Lett. **101**, 107601 (2008).
[23] G. W. Watson, S. C. Parker, and G. Kresse, Phys. Rev. B **59**, 8481 (1999); G. W. Watson and S. C. Parker, J. Phys. Chem. B **103**, 1258 (1999).
[24] D. Le Bellac *et al.*, Phys. Rev. B **52**, 13184 (1995).
[25] J. H. Haeni *et al.*, Appl. Phys. Lett. **78**, 3292 (2001); W. Tian *et al.*, Appl. Phys. Lett. **90**, 022507 (2007).
[26] H. Tanaka and T. Kawai, Appl. Phys. Lett. **76**, 3618 (2000).
[27] P. Fisher *et al.*, Appl. Phys. Lett. **91**, 252901 (2007).